Characterizing and Minimizing Synchronization and Calibration Errors in Inertial Body Sensor Networks

Shanshan Chen, Jeff S. Brantley, Taeyoung Kim, John Lach
Charles L. Brown Department of Electrical and Computer Engineering, University of Virginia
351 McCormick Rd., PO Box 400743
Charlottesville, VA 22904, USA
+1-434-924-6086
{sc2xh, jb7fx, tk2np, jlach}@virginia.edu

ABSTRACT

Body sensor network (BSN) applications depend on accurate and precise data from body-worn devices, but issues related to sensor variations, body mounting variations, and node-to-node synchronization can dramatically impact the quality and reliability of collected data and, ultimately, application fidelity. Characterizing and addressing these sources of error – which are both static and dynamic (e.g. sensors suffer from static manufacturing variability and dynamic environmental impacts) – within the context of application requirements is therefore necessary for the viability of such applications.

This work characterizes and addresses errors related to sensor and mounting calibration and node synchronization on a case study application – knee joint angle as measured during walking by an accelerometer- and gyroscope-based BSN. Using an industrial optical motion capture system to provide ground truth, calibration and synchronization error are quantified and the efficacy of solutions for reducing such errors are evaluated.

1. INTRODUCTION

Body sensor networks (BSNs) have great promise for a number of application domains, but their utility ultimately depends on satisfying fidelity requirements (accuracy, precision, latency, reliability, etc.) specific to their target applications. A number of practical sources of error can affect the accuracy of BSNs, and their effects must therefore be examined in the context of specific applications in order to determine their relative impacts on fidelity. Two critical sources of error across inertial BSN platforms and applications are those relating to synchronization and calibration. Synchronization errors become potentially critical for data fusion from a multi-node system measuring rapidly-changing, non-stationary signals. Calibration errors may occur not only at the sensor level, but also with respect to placement on the body due to body contour variations. While these two types of errors are general across inertial BSN platforms, their impact on fidelity should be characterized in context in order to determine the relative importance of each source for a given application.

To illustrate this, a case study is presented involving the measurement of knee joint angle, a useful metric in gait analysis, using TEMPO 3.1, an inertial BSN platform, with a Vicon® optical motion capture system used for ground truth validation. The effect of synchronization and calibration errors on calculated joint angles is characterized, and methods for addressing and minimizing these errors are discussed and compared. While the error magnitude results are application-specific, the approach for error source characterization and minimization can be applied to any BSN platform and target application.

The rest of this paper is organized as follows. Section 2 details the experimental setup for data collection and analysis. Sections 3 through 5 examine synchronization, sensor calibration, and mounting calibration, respectively, and offer possible solutions for minimizing these errors within the knee joint angle measurement context. Each section presents experimental results showing a relative improvement over the results from the previous sections. Section 6 summarizes the overall analysis in the context of application and concludes the paper.

2. EXPERIMENTAL SETUP

To examine the impact of inertial BSN synchronization and calibration errors within an application context, a case study of knee joint angle measurement is presented. This application typically requires high accuracy but is quite sensitive to synchronization and calibration errors.

2.1 Background

Among the many parameters in gait assessment, knee joint angle is of interest in several clinical research areas, such as osteoarthritis, orthopedics, prosthetics, and knee surgery recovery and rehabilitation. 3D position tracking motion analysis systems such as Vicon® have been developed as standard systems for measuring joint angles in human gait [20], but their immobility limits their use to in-lab data collections. Goniometers have been used as a conventional portable measurement tool for knee angle [10][15], but there are issues of accuracy and wearability.

More recently, inertial BSNs have been developed for continuous, accurate, wearable motion capture [9]. For example, the TEMPO 3.1 system provides six-degrees-of-freedom motion capture on each node in the form factor of a wristwatch [2]. In this paper, the TEMPO 3.1 system, shown in Figure 1 mounted on healthy human subject, was used to measure knee joint angle, with a Vicon® system providing a reference to characterize the error sources present in TEMPO.

2.2 Data Collection

Subjects with no orthopedic or neuromuscular impairment history were mounted with TEMPO nodes and Vicon® markers on each body segment, i.e., left thigh, left shank, right thigh and right shank, as shown in Figure 1(b). Data were taken from the Vicon® and TEMPO systems simultaneously, both sampled at 120 Hz, with a predefined synchronization procedure. All the computation is performed offline, including synchronization achieved by post-processing, calibration, and knee joint angle calculation.

To compute the joint angle correctly, the orientation of sensitive acceleration axes and gyroscope planes relative to the limb must be noted when instrumenting the subject. In this case, the sagittal plane contains the information of interest. Therefore, signals of

the X-axis and Y-axis of accelerometer and the Z-plane of gyroscope were used for computation.

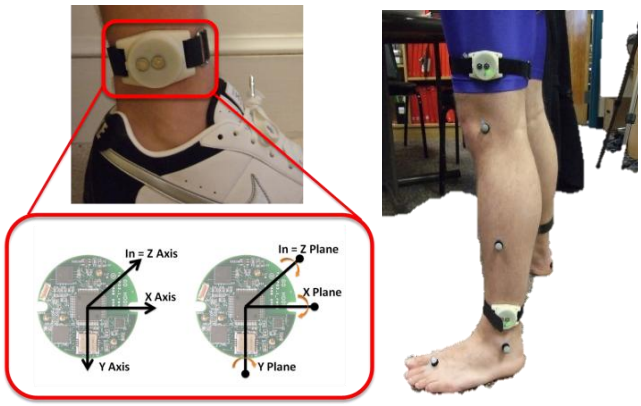

(a) (b)

Figure 1. (a) The TEMPO 3.1 node with mounting position, the TEMPO nodes are placed with the cephalic direction as Y-axis positive, the anterior direction as X-axis positive, and lateral direction as Z-axis positive. (b) The TEMPO nodes mounted on-body.

2.3 Joint Angle Calculation Method

Several researchers have explored ways of measuring joint angle using accelerometer and rate gyroscopes [17][20]. In this paper, an effective yet computationally less intensive method is applied to calculate the knee joint angle by data taken from accelerometer and gyroscope sensors. The knee angle is calculated from the accelerometer data for static postures and from the rate gyroscope data during dynamic walking.

2.3.1 Static joint angle calculation

In the static period, the accelerometers are employed to provide the inclination of each segment. The knee joint angle is obtained by comparing the tilt of the shank and the tilt of the thigh. Following the convention of the Vicon® system, we chose the ground as the reference and subtract the thigh tilt from the shank tilt. The placement of TEMPO nodes is shown in Figure 2.

$$\varphi_{segment} = \arctan\left(\frac{A_x}{\sqrt{A_y^2 + A_z^2}}\right) \quad (1)\ [21]$$

In Equation (1), A_x, A_y, A_z are the linear accelerations obtained from the accelerometer signals with respect to each axis, and $\varphi_{segment}$ is defined as the angle of the X-axis relative to ground. The knee joint angle can be found as,

$$\varphi_{knee} = \left|\varphi_{shank} - \varphi_{thigh}\right| \quad (2)$$

The absolute joint angle is the complement of the angle obtained by Equation (2).

2.3.2 Dynamic joint angle calculation

We obtain dynamic gait period angles by integrating the discrete angular velocity value measured from the rate gyroscope sensors.

$$\varphi[n] = \varphi[n-1] + \frac{\Delta}{2} \times (\omega[n-1] + \omega[n]), \quad (3)\ [17]$$

In Equation (3), ω is the angular velocity obtained from the rate gyroscope signal, Δ is the sampling period ($1/120s$ in this case) and φ is the dynamic angle of each segment with respect to ground. The initial value of the dynamic angle will be obtained from the static posture in every experiment session providing the initial orientation for the gyroscope. The knee joint angle is calculated by subtracting the integrated thigh angle from the integrated shank angle, as shown in Equation (2).

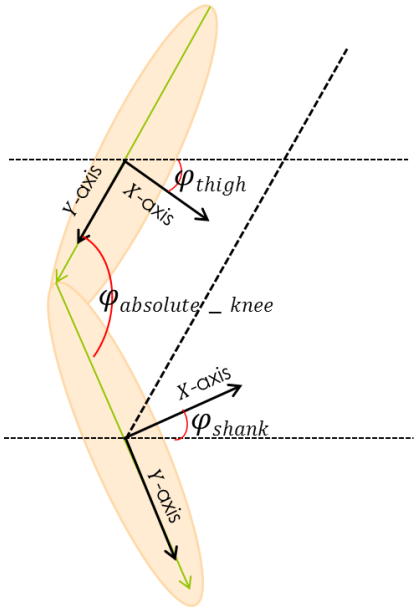

Figure 2. Accelerometer placement and Knee joint angle.

However, this method is subject to error accumulation due to the integration drift caused by the unpredictable gyroscope bias. We apply a high-pass filter to eliminate the drift and offset [17][20]. In this paper, a 3rd order Butterworth high-pass filter with a cut-off frequency of 0.3 Hz is applied. To avoid phase-distortion caused by filtering, the filter is applied twice, forward and backward, to achieve zero-phase distortion [17].

A high-pass filter inevitably removes the DC signal. To compensate this, the knee joint angle obtained from Vicon® is normalized by applying the same high pass filter.

3. SYNCHRONIZATION

BSN applications employing data fusion across multiple sensor nodes can suffer significant error if not properly time-synchronized. Computations combining non-stationary data sample-by-sample from various nodes will, for a given time lag among nodes, incur error related to the rate of change in the signals. For example, a joint angle computed from two limb segment angles will combine segment angles taken at different times and different postures, the degree of which is a function of the time lag between signals and the speed of the limb motion.

3.1 Synchronization Methods

3.1.1 Network-based synchronization

Achieving time synchronization is a matter of both reconciling the time offset between nodes at a given time instant, as well as accounting for subsequent clock drift due to slight variations in clock frequency among nodes [19]. Some form of message passing can correct the time offset, but errors can result from

various uncertain delays as follows: the delay between message creation and arrival at the MAC layer (send time), the MAC layer delay until transmission (access time), the over-the-air transmission delay (propagation time), and the delay to receive the length of the message (receive time) [18].

Numerous synchronization methods have been proposed in the wireless sensor network (WSN) community. Reference Broadcast Synchronization (RBS) eliminates error due to send time and access time by broadcasting a message from one master node to all neighbors at once, which then compare receipt times. The Timing-synch Protocol for Sensor Networks (TPSN) and Flooding Time Synchronization Protocol (FTSP) minimize delay errors by timestamping messages at the MAC layer, and they are also designed to scale with multi-hop networks, with FTSP being more robust to topology changes [8][14].

A number of other methods are surveyed in [19], which identifies some criteria for selection of an appropriate synchronization method, including energy requirements, network size, topology variability, and necessary synchronization precision. Yet, for a small, one-hop network BSN streaming data to a single aggregator at high data rates, the requirements may be less stringent than for WSNs, and so the best method may simply be that which is already implemented or most easily implemented on the chosen platform.

3.1.2 Sensor event-based synchronization

The above methods, however, depend on message broadcast support or access to MAC-layer timing information, but this may not always be the case. For instance, the TEMPO system incorporates a commodity RFCOMM-enabled Bluetooth radio, such as could be used to communicate with recent Android-based smartphones, which support only basic RFCOMM Bluetooth communication.

One solution is to instead synchronize the aggregated data based on intentionally generated sensor events. The BSN user performs some synchronization action that applies stimuli simultaneously to multiple sensors. An operator can manually note the times of the sensor events during post-processing. [1] describes the use of "spotting" algorithms for automatic detection of these events in multimodal sensor environments, and advocates repeating the synchronization action multiple times to avoid errors from false detections.

A simpler approach can suffice for synchronizing sensor streams recorded by the same type of sensor. If the time window of the synchronization action is recorded by an operator via aggregator software, offline processing can automatically examine this window to determine the lag between streams. The time lag (as a number of samples) between the two streams is that which maximizes the cross-correlation between them. Since the measurement and adjustment of time lag can be performed offline, this approach requires no firmware modifications to the BSN platform.

Event-based synchronization can be useful not only for synchronization within a BSN, but between BSNs that are not necessarily programmed to interoperate. Furthermore, it can be used to synchronize against a non-BSN system, such as an optical motion capture system for ground-truth validation of an inertial BSN experiment, but manual spotting of the events may be necessary. For example, in this study, synchronization between the TEMPO and Vicon® systems was achieved by striking a TEMPO node against a Vicon® system force plate. Similarly, video recordings of experiments can be synchronized to BSN data by selecting the video frame during which a synchronization action occurred.

3.2 Joint Angle Error Due to Time Lag

The joint angle calculation in Equation (2) involves a subtraction between angles derived from separate nodes on a sample-by-sample basis. For a time lag of m samples between the thigh and shank nodes, segment angles occurring $m\Delta$ seconds apart are compared.

The resulting error was extrapolated from the experimental gait data for a range of time lags between the shank and thigh nodes, from -2s to +2s in $1/\Delta$ s increments. The resulting RMSE depends on the gait speed. For a given lag, the shank and thigh are farther apart in the gait cycle at faster gait speeds. Also, the RMSE is periodic with a period equal to the gait period.

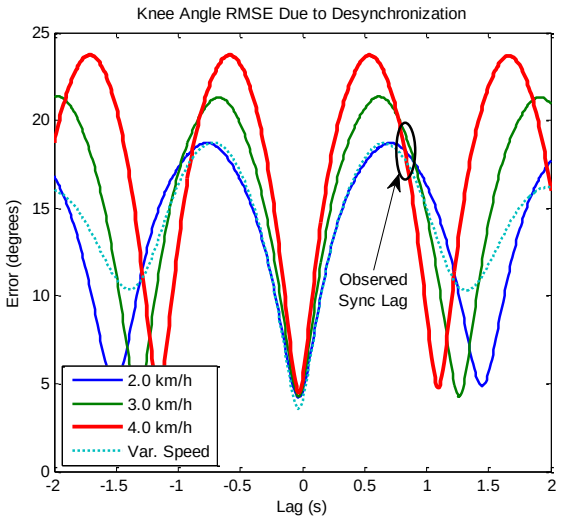

Figure 3. Knee angle RMSE for simulated -2s to +2s lag.

The knee angle RMSE is shown in Figure 3. The RMSE is minimized at zero lag, where there remains a roughly 4° error, to be addressed in subsequent sections. The highlighted data points correspond to the actual lag observed in this trial between the shank and thigh nodes. This rather large lag results in an increase of about 17° in the RMSE relative to the synchronized case. A medium-speed gait reaches a 5° increase in RMSE around a 100 ms lag, but a lag around 15 ms can be tolerated to within 1°. Certainly any synchronization method guaranteeing a 1 ms precision or less would be sufficient for this application. Other applications may require greater or lesser synchronization precision.

4. SENSOR CALIBRATION

Accelerometers and rate gyroscopes used in inertial BSN platforms are typically assumed to follow a linear model. The relationship between the sensed quantity, M, and the output voltage, V, is described by Equation (4), which contains two key parameters: the sensitivity, S, and the offset, O.

$$M = \frac{(V - O)}{S} \qquad (4)$$

The sensitivity is the ratio of voltage change to change in the physical quantity, and the offset is the output voltage when no motion (or gravitational field, in the case of accelerometers) is applied to the sensor. These parameter values can be found in the sensor datasheets, but in practice they will deviate from the expected value.

Sources of sensor error include manufacturing variations and environmental conditions, such as temperature, meaning that sensitivity and offset will vary both across different sensors at a given time, or within a single sensor at various times. Datasheets and white papers from manufacturers additionally list other possible error sources, such as nonlinearity, non-orthogonality between axes, and cross-axis sensitivity. Finally, variations in chip mounting on a PCB or mounting of the PCB in the node packaging can place the sensing axes slightly out of the assumed frame of reference.

4.1 Methods

It is impractical to individually compensate for these sources of error, and so some form of calibration is employed to holistically minimize their effect. The sensor response is checked against a known reference point (such as the gravitational field or a turntable) in order to calculate the actual sensitivity and offset by linear mapping or Newton's method [3][7][11][13]. Others have also attempted to use Kalman filtering [12], a method conventionally used in GPS, but it was not able to meet the requirements for on-body application fidelity. This section evaluates three different calibration techniques both on- and off-body.

4.1.1 Linear mapping technique

The simplest calibration technique is the linear mapping of two points measured with respect to gravity into the linear function of Equation (4). The sensitivity and offset are calculated from these reference points according to Equation (5).

$$\begin{cases} Sensitivity = \frac{V_{max} - V_{min}}{2} \\ Offset = \frac{V_{max} + V_{min}}{2} \end{cases} \quad (5)$$

For accelerometers, each axis of sensor is exposed to 1g and -1g by placing it parallel with gravity. Similarly, rate gyroscope sensors can be placed on a turntable and subjected to the available rotational rates, typically 33 RPM and 45 RPM.

4.1.2 Mathematical estimation technique

The mathematical estimation technique is based on the principle that the sum of vector magnitude of 3-axes' accelerations is 1g when the accelerometer is stationary. This technique only applies for accelerometers. This principle is described by Equation (6)

$$\sqrt{\alpha_x^2 + \alpha_y^2 + \alpha_z^2} = 1g \quad (6)$$

The three-axis accelerometer sensor is subjected to the gravitational field in six arbitrary orientations (rather than with each axis subsequently placed parallel with gravity). Each set of measurements, M_x, M_y, M_z, gives rise to an equation of the form given by Equation (7), where S_i and O_i are the sensitivity and offset, respectively, of axis i.

Once the accelerometer output with 6 arbitrary orientations are obtained, it can be solved by mathematical iterative estimation such as the Newton-Raphson method. The equation is given as follow:

$$F(S_x, S_y, S_z, O_x, O_y, O_z) = \sqrt{\frac{M_x - O_x}{S_x} + \frac{M_y - O_y}{S_y} + \frac{M_z - O_z}{S_z}} - 1 = 0 \quad (7)$$

This system of six equations can be solved for the sensitivities and offsets by a mathematical iterative estimation, such as the Newton-Raphson method. An arguable advantage of this technique is that it does not require a perfectly level surface for calibration, but it does require an initial computational complexity due to the iterative estimation [13].

4.1.3 Piecewise mapping technique

The previous techniques assume a linear sensor model, but a piecewise linear equation may better fit the nonlinearities in the sensor response. This procedure requires profiling the sensor against more than two known reference points and mapping the readings into a piecewise linear function. For an n-point linear function, the n^{th} sensitivity and offset are given as follows:

$$\text{Sensitivity(n)} = \frac{(V_n - V_{n-1})}{\cos\theta_n - \cos\theta_{n-1}}, \text{Offset} = \frac{V_n + V_1}{2} \quad (8)$$

with n being the number of required measurement points. The most convenient and commonly used method is 3 data points, such as 0°, 90°, and 180°. However, increasing the number of data points increases the conversion accuracy, as detailed in the following section.

4.2 Calibration Experiment

4.2.1 Off-body analysis

In order to accurately test and measure angles obtained by accelerometer data, a digital inclinometer instrument with ±0.5° error was used. A typical turntable with two constant speed settings (200°/s, 270°/s) were used for gyroscope calibration and verification. Figure 4 shows the experiment setup of accelerometer and gyroscope for calibration and measurement.

Figure 4. Calibration and measurement instrument

The TEMPO node is pictured in a custom bracket used to precisely place it in the desired frame of reference.

Table 1 shows a comparison among 4 calibration methods for the accelerometer, including piecewise mapping with n = 3, 5, and 7. Datasheet conversion refers to the baseline case using the sensitivity and the offset listed in the sensor datasheet. In order to verify the output, the measurement was performed at10° increments from 0° to 180° on the inclinometer. Piecewise calibration results in the lowest RMSE, with more data points providing higher accuracy, although the additional efforts to obtain a high n must be balanced against the accuracy improvements.

Table 1. Accuracy analysis of 1-axis calibrated accelerometer

Calibration Techniques	RMSE	Mean of Angle Error (deg)
Datasheet Conversion	22.75	20.95
Newton	1.63	0.26
Linear	1.53	0.24
Piecewise(n=3)	1.51	0.22
Piecewise(n=5)	0.78	0.20
Piecewise(n=7)	0.70	0.15

The accuracy of the gyroscope sensor using both linear and piecewise mapping (n=3), are shown in Table 2. The gyroscope was profiled at 270°/sand tested at 200°/s. Both methods show similar improvement over the baseline (datasheet value) case.

Table 2. Verification of two gyroscope calibration

Sensors	Calibration Techniques	Angular Velocity (°/s)	
		+200°/s	**-200°/s**
ADXRS300 X- and Y-Axis	**Datasheet (No calibration)**	190.9±0.66	-174.5±0.59
	Linear	204.3±0.73	-194.8±0.64
	Piecewise(n=3)	204.2±0.73	-196.5±0.64
IDG-300 Z-Axis	**Datasheet (No calibration)**	163.4±0.56	-230±0.58
	Linear	199.2±0.58	-206.5±0.60
	Piecewise(n=3)	200±0.58	-207.1±0.60

4.2.2 On-body analysis

TEMPO nodes were mounted on human subjects as stated in Section 2, for the purpose of verifying the calibration in the context of knee joint angle measurement. Of the above-described calibration techniques were tested for static and dynamic knee joint angle measurement and compared against results from the Vicon® system. All data was synchronized using the technique stated in Section 3.

Table 3. Static knee joint angle between Vicon® and TEMPO

Vicon®	TEMPO Angle Error (deg)			
	Datasheet Conv.	**Linear Calib.**	**Newton Raphson**	**Piecewise Calib.(n=3)**
0.66	12.37	8.22	6.16	9.73
54.76	25.32	15.70	18.14	16.88
65.21	24.24	15.36	17.51	16.21
83.32	25.01	17.60	19.05	17.8
104.09	33.73	31.13	32.07	30.84

Table 3 shows the results of static knee joint angle measurement using accelerometers corresponding to different postures. Although error is minimized with the best calibration method (piecewise) as shown in the off-body analysis, the errors are tremendously increased when put on-body, which may even disguise the impact of calibration

Table 4. Dynamic knee joint angle RMSE (in degrees) comparing Vicon® and TEMPO

Gait Speed (km/h)	Measurement Error (RMSE)		
	Datasheet	**Linear**	**Piecewise(m=3)**
2	8.72	2.75	3.59
3	9.51	3.03	3.88
4	9.87	3.15	4.01
Various speed	8.96	2.86	3.67

The results of the dynamic joint knee angle analysis are shown in Table 4. The measurements were taken at different gait speeds: constant speeds of 2 km/h, 3 km/h, and 4km/h, as well as a varying-speed trial. While calibration still results in an improved RMSE compared to using only datasheet-supplied values, there is a large error compared to the off-body tests, which may be attributed to mounting error, as discussed in the next section.

5. MOUNTING CALIBRATION

Mounting error has emerged as the dominant error source in this application, resulting in a large knee angle error even after other errors have been minimized. In this section, we investigate various mounting errors in inertial BSNs affecting both accelerometers and rate gyroscopes and evaluate correction methods for different mounting errors.

5.1 Static Mounting Error Compensation

While the calculation of knee angle during static periods (i.e. no movement) should be easily derived from the analysis in Section 2.3.1, mounting error introduces significant inaccuracies, including errors up to 30.8 degrees (see Table 3). The tilt detection mechanism of accelerometers brings up a trade-off in static angle measurement. On one hand, the accelerometers are sensitive to detect the tilt when precisely positioned. On the other hand, this sensitivity makes them prone to "noisy" tilt introduced by body shape instead of segment inclination.

We identify the mounting errors affecting accelerometers as following:

1. When the motion sensor is mounted on a human body, the axes of acceleration can be shifted and rotated from the assumed orientations due to the nodes becoming mis-positioned on the body or rotated via muscle flexion and extension. Therefore, calculating the angle with respect to the assumed coordinate results in an error.
2. The specific reference points for knee joint angles calculation are different for Vicon® and TEMPO. The Vicon® system captures the anatomy of the human subjects and produces knee joint angle as the angle between the femur and tibia bones, while TEMPO system are mounted on skin where the angle is similar but not equivalent to the bone-to-bone knee angle, which leaves a discrepancy with the angle measured by reference system.

The inaccuracies seen in Table 3 include both of these error sources. A simple approach to compensating for these errors is to use a point to determine an offset magnitude that is then used to adjust the other calculated angles. By doing this, we improved the accuracy with an average residual error of 10.7 degrees.

5.2 Dynamic Mounting Error Compensation

The dynamic knee joint angle retrieved from the rate gyroscope sensed angular velocity is affected by mounting error as well. Comparing with mounting error affecting accelerometer data, we found:

1. Data from the z-plane gyroscope does not change if the gyroscope is rotated on the z-plane, and the mounting orientation does not affect the gyroscope data as badly as the accelerometer data.
2. The gyroscope recorded knee joint angle signal attenuates comparing to the reference signal due to the anatomy capture difference.
3. With a careful inspection of the human gait, it is noticeable that during walking, though most of the swing motions locate on sagittal plane, subtle rotations happen on other planes too [16]. Therefore, using only the z-plane gyroscope signal, the limb rotation and the final knee joint swing range will be attenuated as shown in Figure 5 (comparing "TEMPO" to "Vicon®").

Because of the complexity of the gait motion, further study and more refined modeling are required to compensate for mounting error. For example, a general solution for error compensation in periodical gait signals leverages the fact that the error waveforms (i.e. Vicon® vs. TEMPO) are also periodic with the gait cycle, as plotted in Figure 5 ("Error before Compensation"). It is therefore possible to characterize the error for a number of gait cycles and then apply a compensating signal to all subsequent cycles. In this paper, we average the error taken from 25 cycles within each speed session and add this averaged cyclic error to the original knee joint angle of each gait cycle. It is clear in Figure 5 that the resulting "Compensated Joint Angle" nearly matches Vicon®.

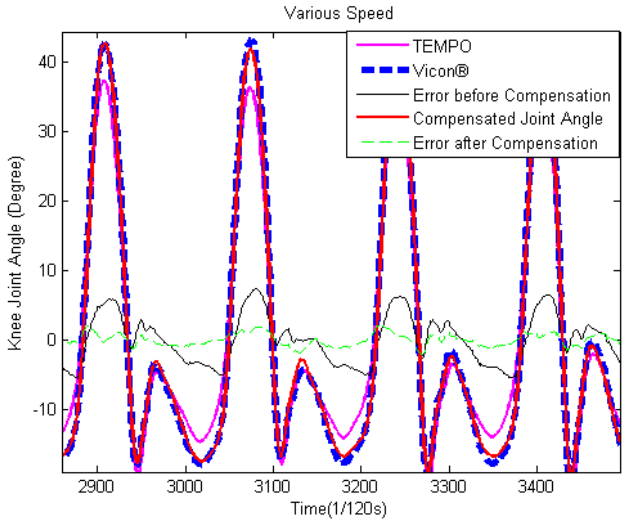

Figure 5 Cyclic Error Compensation Method

Table 5 Improved accuracy after cyclic error compensation method

Gait Speed	Without error Compensation		With Error Compensation	
	Coefficient	RMSE	Coefficient	RMSE
2km/h	0.9935	2.70	0.9950	1.65
3km/h	0.9930	3.00	0.9969	1.40
4km/h	0.9919	3.14	0.9962	1.61
Various speed	0.9911	2.79	0.9959	1.51

Table 5 shows that after applying the cyclic error, the average correlation between the TEMPO measured knee joint angle and Vicon® has increased from 0.9924 to 0.9960, and the average RMSE has reduced from 2.91 degrees to 1.54 degrees. Comparing with the results achieved in [20], which gives a correlation of 0.98 and RMSE of 3.98 degrees, the improvement thanks to the error characterization has been shown.

This cyclic error compensation method must be validated against different subjects and speeds. It may also conceal the possible controllable sources of errors. Therefore, it should be only used after all of the other error sources in the system have been minimized.

6. CONCLUSION

While the synchronization and calibration error sources discussed in this paper are inherent in any BSN, it is essential to characterize the fidelity impact of such errors on the target application. While such analysis is application-specific (and must therefore be repeated for each application), it is essential for achieving required application fidelity with emerging BSN platforms.

In this paper, node synchronization, sensor calibration, and mounting calibration error sources were characterized for knee joint angle measurement (common in physical rehabilitation and gait research) using TEMPO, a multi-node inertial BSN. An industrial optical motion capture system was used for quantifying error and evaluating the effectiveness of various methods for minimizing error. The error sources were determined to have significantly different effects on application fidelity. Mounting calibration proved to be the biggest challenge, but compensation methods were explored that provided accuracy up to an RMSE of ~1.5 degrees during walking, which is within the range of error in the optical motion capture system.

Future work includes both application-specific efforts to maximize the fidelity of motion analysis using inertial BSNs and the development of a generic framework for connecting low-level error sources to ultimate application fidelity.

7. REFERENCES

[1] Bannach, D., Amft, O., and Lukowicz, P. Automatic event-based synchronization of multimodal data streams from wearable and ambient sensors. *Smart Sensing and Context: 4th European Conference, EuroSSC 2009*, Springer (2009), 135-148.

[2] Barth, A., Hanson, M., Powell Jr, H., and Lach, J. TEMPO 3.1: A Body Area Sensor Network Platform for Continuous Movement Assessment. *Proceedings of the 2009 Sixth International Workshop on Wearable and Implantable Body Sensor Networks-Volume 00*, IEEE Computer Society (2009), 71–76.

[3] Borenstein, J., Ojeda, L., and Kwanmuang, S. Heuristic reduction of gyro drift in IMU-based personnel tracking systems. *Proceedings of SPIE 7306*, (2009), 73061H-73061H-11.

[4] Camps, F., Harasse, S., and Monin, A. NUMERICAL CALIBRATION FOR 3-AXIS ACCELEROMETERS AND MAGNETOMETERS. *Electro/Information Technology, 2009. eit '09. IEEE International Conference on*, Ieee (2009), 217-221.

[5] Elson, J., Girod, L., and Estrin, D. Fine-grained network time synchronization using reference broadcasts. *ACM SIGOPS Operating Systems Review 36*, (2002), 147–163.

[6] Freescale Semiconductor, *Accelerometer Terminology Guide*, 2007.

[7] Frosio, I., Pedersini, F., and Borghese, N.A. Autocalibration of MEMS Accelerometers. *Instrumentation and Measurement, IEEE Transactions on*, (2009), 2034-2041.

[8] Ganeriwal, S., Kumar, R., and Srivastava, M. Timing-sync protocol for sensor networks. *Proceedings of the 1st international conference on Embedded networked sensor systems*, ACM (2003), 149.

[9] Gouwanda, D. and Senanayake, S. Emerging Trends of Body-Mounted Sensors in Sports and Human Gait Analysis. *Springer*, (2008), 2008-2008.

[10] Johnson, F., Watts, W., and Evans, D. Goniometer for continuous recording of knee angle. *Medical and Biological Engineering and Computing 19*, 2 (1981), 255–256.

[11] Krohn, A., Beigl, M., Decker, C., Kochendörfer, U., Robinson, P., and Zimmer, T. *Inexpensive and Automatic Calibration for Acceleration Sensors*. 2005.

[12] Luinge, H.J. and Veltink, P.H. Inclination measurement of human movement using a 3-D accelerometer with autocalibration. *Neural Systems and Rehabilitation Engineering, IEEE Transactions on 12*, 1 (2004), 112-121.

[13] Lukowicz, P., Junker, H., and Tröster, G. Automatic Calibration of Body Worn Acceleration Sensors. *Pervasive Computing*, (2004), 176-181.

[14] Maróti, M., Kusy, B., Simon, G., and Lédeczi, Á. The flooding time synchronization protocol. *Proceedings of the 2nd international conference on Embedded networked sensor systems*, ACM New York, NY, USA (2004), 39–49.

[15] Oberg, T., Karsznia, A., and Oberg, K. Joint angle parameters in gait: reference data for normal subjects, 10-79 years of age. *Journal of rehabilitation research and development 31*, 3 (1994), 199.

[16] Ross Bogey, D. Gait Analysis. (2009), http://emedicine.medscape.com/article/320160-overview,

[17] Salarian, A., Russmann, H., Vingerhoets, F.J., et al. Gait assessment in Parkinson's disease: toward an ambulatory system for long-term monitoring. *IEEE transactions on bio-medical engineering 51*, 8 (2004), 1434-43.

[18] Sivrikaya, F. and Yener, B. Time synchronization in sensor networks: a survey. *IEEE Network 18*, 4 (2004), 45-50.

[19] Sundararaman, B., Buy, U., and Kshemkalyani, A.D. Clock synchronization for wireless sensor networks: a survey. *Ad Hoc Networks 3*, 3 (2005), 281-323.

[20] Tong, K. and Granat, M.H. A practical gait analysis system using gyroscopes. *Medical engineering & physics 21*, 2 (1999), 87-94.

[21] Tuck, K. and Tempe, A. Tilt sensing using linear accelerometers. *Freescale Semiconductors Inc. application note AN3461*, (2007).

[22] Young, A.D. Comparison of Orientation Filter Algorithms for Realtime Wireless Inertial Posture Tracking. *Wearable and Implantable Body Sensor Networks, 2009. BSN 2009. Sixth International Workshop on*, (2009), 59-64.